ELSEVIER

Journal of Nuclear Materials 296 (2001) 145–154

journal of nuclear materials

www.elsevier.com/locate/jnucmat

Correlation of radiation-induced changes in mechanical properties and microstructural development of Alloy 718 irradiated with mixed spectra of high-energy protons and spallation neutrons

B.H. Sencer [a,b,*], G.M. Bond [a], F.A. Garner [b], M.L. Hamilton [b], S.A. Maloy [c], W.F. Sommer [c]

[a] *New Mexico Institute of Mining and Technology, Socorro, NM 87801, USA*

[b] *Materials Resources Department, Pacific Northwest National Laboratory, P.O. Box 999, Building #326, Battelle Boulevard, P8-15, Richland, WA 99352, USA*

[c] *Los Alamos National Laboratory, Los Alamos, NM 87545, USA*

Abstract

Alloy 718 is a $\gamma'(Ni_3(Al, Ti))$–$\gamma''(Ni_3Nb)$ hardenable superalloy with attractive strength, and corrosion resistance. This alloy is a candidate material for use in accelerator production of tritium (APT) target and blanket applications, where it would have to withstand low-temperature irradiation by high-energy protons and spallation neutrons. The existing data base, relevant to such irradiation conditions, is very limited. Alloy 718 has therefore been exposed to a particle flux and spectrum at the Los Alamos Neutron Science Center (LANSCE), closely matching those expected in the APT target and blanket applications. The yield stress of Alloy 718 increases with increasing dose up to ~0.5 dpa, and then decreases with further increase in dose. The uniform elongation, however, drastically decreases with increasing dose at very low doses (<0.5 dpa), and does not recover when the alloy later softens somewhat. Transmission electron microscopy (TEM) investigation of Alloy 718 shows that superlattice spots corresponding to the age-hardening precipitate phases γ' and γ'' are lost from the diffraction patterns for Alloy 718 by only 0.6 dpa, the lowest proton-induced dose level achieved in this experiment. Examination of samples that were neutron irradiated to doses of only ~0.1 dpa showed that precipitates are faintly visible in diffraction patterns but are rapidly becoming invisible. It is proposed that the γ' and γ'' first become disordered (by <0.6 dpa), but remain as solute-rich aggregates that still contribute to the hardness at relatively low dpa levels, and then are gradually dispersed at higher doses. Published by Elsevier Science B.V.

1. Introduction

An understanding of the response of candidate materials to the irradiation conditions they would experience in the accelerator production of tritium (APT) facility is essential to proper development of APT components [1]. No information was previously available for application of Alloy 718 in such severe conditions. Such spallation environments produce high radiation damage levels, concurrent with high rates of helium and hydrogen generation, at relatively low irradiation temperatures. The data already available were derived, in general, from situations involving relatively low particle energies, much lower gas (He/H) generation rates, and much lower doses, compared to those expected in APT.

Therefore, specimens of APT candidate materials were irradiated at 800 MeV 100 mA LANSCE accelerator, to relatively low exposures in neutron furnaces, and to displacement levels as high as ~15 dpa in the direct proton beam in order to simulate APT conditions

* Corresponding author. Tel.: +1-509 376 0156; fax: +1-509 376 0418.

E-mail address: bulent.sencer@pnl.gov (B.H. Sencer).

0022-3115/01/$ - see front matter. Published by Elsevier Science B.V.
PII: S0022-3115(01)00517-7

[1]. Nevertheless, even the high-exposure data obtained will have to be extrapolated to doses 2–3 times higher in order to predict materials performance in APT conditions for its expected service life. A good understanding of the microstructural changes responsible for changes in mechanical behavior is essential, if the mechanical property data are to be extrapolated to higher exposures with confidence.

Changes in tensile properties of Alloy 718 irradiated in the mixed proton and spallation neutron spectra at LANSCE have been reported elsewhere [2,3]. The yield stress of Alloy 718 increases rapidly with increasing dose up to ~0.5 dpa, and then decreases slowly thereafter with further increases in dose as shown in Fig. 1. The uniform elongation, however, decreases drastically at very low doses (<0.5 dpa), and does not recover even when the alloy later softens somewhat. Helium and hydrogen measurements on Alloy 718 have also been reported [4,5]. The retained helium increases continuously at a rate of ~150 appm/dpa while the hydrogen retention is ~50–100% higher as shown in Fig. 2. For instance, in Alloy 718, ~1830 appm helium and ~5000 appm hydrogen were retained at 13.4 dpa.

To investigate the microstructural evolution of the materials in a mixed proton and spallation neutron environment, specimens ranging between 0.1 and 13.4 dpa were examined by transmission electron microscopy (TEM). The present paper describes the radiation-induced microstructural evolution of Alloy 718 and its role in the concurrent changes in mechanical properties.

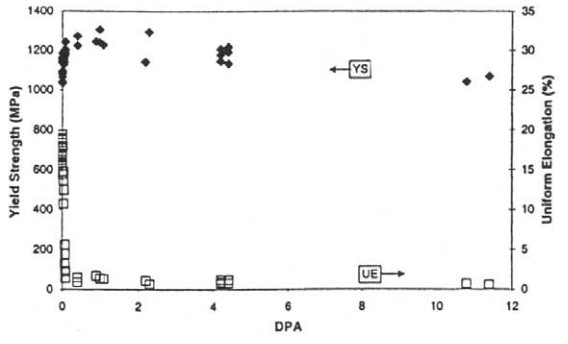

Fig. 1. Yield strength (solid symbols) and uniform elongation (open symbols) of Alloy 718 irradiated at low temperatures and tested at 20–164°C [2].

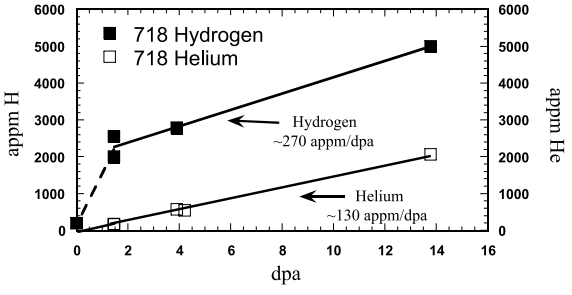

Fig. 2. Measured helium and hydrogen retention of Alloy 718 [4,5].

2. Experimental conditions

The heat of Alloy 718 used in this study had the following composition: 53.58%Ni, 18.37%Fe, 18.13%Cr, 4.98%(Nb + Ta), 3.06%Mo, 1.03%Ti, 0.11%Si, 0.48%Al, 0.13%Mn, 0.08%Cu, 0.04%C, 0.001%S, 0.008%P (in wt%). Alloy 718 specimens were electro-discharge-machine (EDM) cut from the as-received material (annealed condition), then wrapped in Nb foil and encapsulated in a quartz tube (evacuated and back-filled with Ar). The specimens were then heat treated with the following steps: annealed at 1065°C for 30 min and air cooled, aged at 760°C for 10 h, furnace cooled to 650°C and held for a total time of 20 h, with a final air cool to room temperature.

The irradiation was conducted in LANSCE at Los Alamos National Laboratory. Details of the irradiation were published previously [1]. In this specimen series there was a Gaussian proton flux having a circular profile in intensity with $2-\sigma = 3$ cm over the specimen ensemble. Doses were determined through analysis of the isotopes produced in activation foils placed alongside the specimens [6]. The irradiation temperatures were determined from thermocouples placed in each reference tube [7]. Irradiated specimens were chosen for microstructural evaluation depending on the proton beam intensity at their location. The irradiation temperature varied somewhat with position and dose rate, such that the temperature was ~72°C at the lowest out-of-beam dose, 0.1 dpa, and ~32–55°C at 0.6 and 13.4 dpa, respectively.

Thin-foil samples of Alloy 718 were prepared for TEM examination by conventional jet electropolishing methods, in 5% perchloric acid, 95% ethyl alcohol at −25°C and 55 V. TEM examinations were conducted with a JEOL 2010F (FEG-STEM, 200 keV) for high-resolution, and a JEOL 2000E (200 keV) for the diffraction-contrast microstructural characterization and energy-dispersive X-ray spectrometry (EDS).

3. Results

3.1. Microstructural evolution of Alloy 718

3.1.1. Unirradiated condition

Alloy 718 is a γ'–γ'' age-hardenable alloy. It develops high strength during thermal aging by precipitating

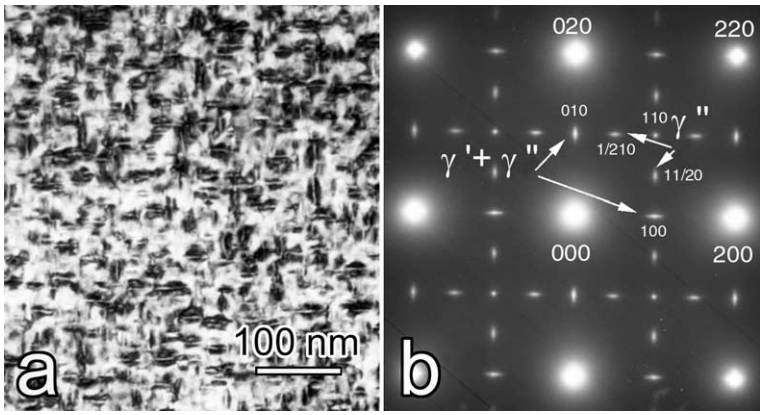

Fig. 3. (a) BF image of unirradiated Alloy 718, and (b) [0 0 1] electron diffraction pattern showing the superlattice reflections.

finely dispersed Ni_3Nb-γ'' and $Ni_3(Ti, Al)$-γ' in an austenitic γ matrix. The γ' and γ'' phases represent ordered variations of the fcc lattice. γ' has a cubic $L1_2$ ordered structure based on Ni_3Al, with Ti and some Nb substituting on Al sites. γ'' has a tetragonal DO_{22} ordered structure based on Ni_3Nb, with minor Al and Ti substitutions on the Nb sites. From consideration of the Nb, Al, and Ti sites, it is apparent that the DO_{22} structure can also be described as having body-centered tetragonal (bct) symmetry, while the $L1_2$ structure can be considered as having cubic symmetry. The γ'' precipitates have a disc-shaped morphology, while γ' particles are spheroidal. The γ'' precipitates have a definite orientation relationship with the austenitic γ matrix: $(0\,0\,1)_{\gamma''}//\{0\,0\,1\}_{\gamma}$ and $[1\,0\,0]_{\gamma''}//\langle 1\,0\,0\rangle_{\gamma}$ [8,9].

As shown in the bright-field (BF) image in Fig. 3(a), the high density of precipitates (γ' and γ'') and the excessive coherency strain contrast around individual particles make them difficult to resolve. A typical [0 0 1] diffraction pattern is also shown in Fig. 3(b). The γ' and γ'' precipitates can be clearly shown by dark-field (DF) analysis with specific superlattice reflections. Reflections of the type (1 0 0), (0 1 0) and (1 1 0) could arise from either γ' or specific variants of the γ''. The γ' superlattice reflections in this pattern have been indexed with respect to the fcc matrix. Reflections of the form (11/20) are allowed for the DO_{22} bct phase, but not for γ'. Thus, the observation of such reflections in Fig. 3(b) clearly demonstrates that a bct γ'' precipitate is present.

A systematic DF analysis is shown in Fig. 4. Here the (0 1 0), (1/210), (1 1 0), (11/20) and (1 0 0) reflections were used. These DF images (all from the same section of grain in the foil) are shown along with their corresponding diffraction patterns. The (0 1 0), (1 1 0) and (1 0 0) DF images (Figs. 4(b) (d) and (f)) clearly reveal the presence of three different variants of a fine, disc-shaped precipitate. In Figs. 4(b) and (f), two different variants are lying along the (1 0 0) and (0 1 0) planes. The third variant, lying in the (0 0 1) plane of the foil, is visible in Fig. 4(d). The orientation and selective imaging of the different precipitate variants are consistent with the bct γ''. The (1/210) and (11/20) DF images (Figs. 4(c) and (e)) identify the disc-shaped precipitate as bct γ''.

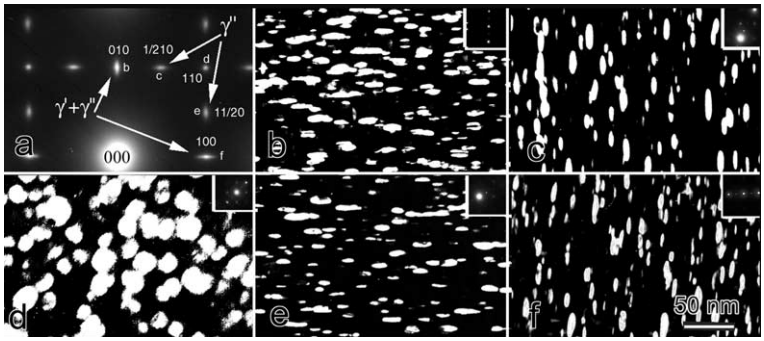

Fig. 4. Unirradiated Alloy 718 [0 0 1] orientation: (a) electron diffraction pattern of [0 0 1]; DF micrographs with (b) $g = (0\,1\,0)$ $(\gamma' + \gamma'')$; (c) $g = (1/210)$ (γ''); (d) $g = (1\,1\,0)$ $(\gamma' + \gamma'')$; (e) $g = (11/20)$ (γ''); (f) $g = (1\,0\,0)$ $(\gamma' + \gamma'')$.

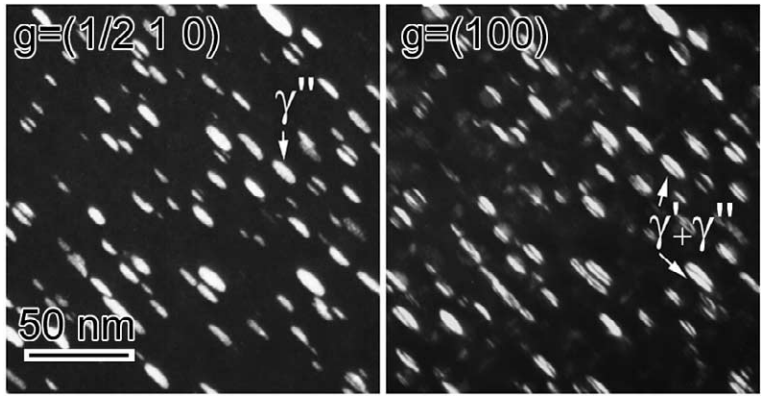

Fig. 5. Unirradiated Alloy 718, DF micrographs with $g = 1/210$ (γ'') and $g = (1\,0\,0)$ ($\gamma' + \gamma''$) from the same area of the grain.

The [1 0 0] γ'' variant is imaged with both the (1 0 0) and (1/210) reflections (Figs. 4(c) and (f)) while the [0 1 0] variant is imaged with the (0 1 0) and (11/20) reflections (Figs. 4(b) and (e)). The existence of γ' can also be seen by comparison of the DF images produced by, for example, (1/210) and (1 0 0) superlattice reflections, as shown in Fig. 5.

Lattice imaging of the unirradiated Alloy 718 confirmed that the intragranular γ' and γ'' particles occur in pairs, each γ' particle sharing an interface with a γ'' particle. In the [0 0 1] lattice image shown in Fig. 6, the γ' is distinguished from the fcc matrix by its doubled lattice spacing. The γ'' has a different structure, and shows evidence of coherency strain along its interface with the matrix.

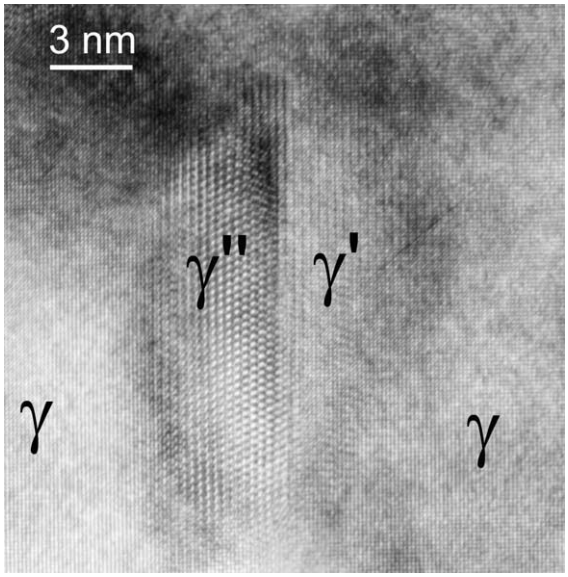

Fig. 6. High-resolution electron micrograph of unirradiated Alloy 718. [0 0 1] lattice image showing γ'–γ'' precipitates.

TEM–EDS analysis was performed on unirradiated Alloy 718 samples in order to identify the carbides that are also present in the material. Because electropolished thin-foil TEM samples are random sections through material containing embedded precipitate particles with widely varied sizes, the particle analysis generally contains contributions from an unknown thickness of superimposed matrix material. The results of compositional analysis for representative particles that appeared nearly free of matrix contributions indicated that the particles were Nb-rich carbides with an average composition of 80–87%Nb, 7–11%Ti, 2–7%Ni, 1–3%Fe, 1–3%Cr, 0–2%Mo, <0.5%Al, Si in wt%.

3.1.2. Irradiated Alloy 718

γ' and γ'' phase instability. γ' and γ'' phases in Alloy 718 exhibited instabilities under proton irradiation between 32°C and 55°C. After doses as low as 0.6 dpa, all evidence of the γ' and γ'' particles in the matrix had disappeared from the electron diffraction patterns. As shown in Fig. 7, the γ' and γ'' superlattice diffraction spots, clearly evident for unirradiated samples, were absent after irradiation. No other precipitate spots (that would correspond to irradiation-induced phases) appeared in electron diffraction patterns from the irradiated samples.

In order to investigate further the disappearance of the γ' and γ'', samples of Alloy 718 were examined that had been neutron irradiated to a lower dose of ~0.1 dpa at ~72°C. γ' and γ'' reflections were still faintly visible in the diffraction patterns, as demonstrated by Fig. 8 in which diffraction patterns from unirradiated and ~0.1 dpa samples are compared. As seen in Fig. 9, precipitate DF images from these reflections confirmed that the precipitates were still present, although they gave a more patchy, discontinuous contrast.

Radiation-induced defects. {1 1 1}-faulted dislocation loops, i.e., Frank loops, were present at all dpa levels. In the case of neutron-irradiated samples (~0.1 dpa),

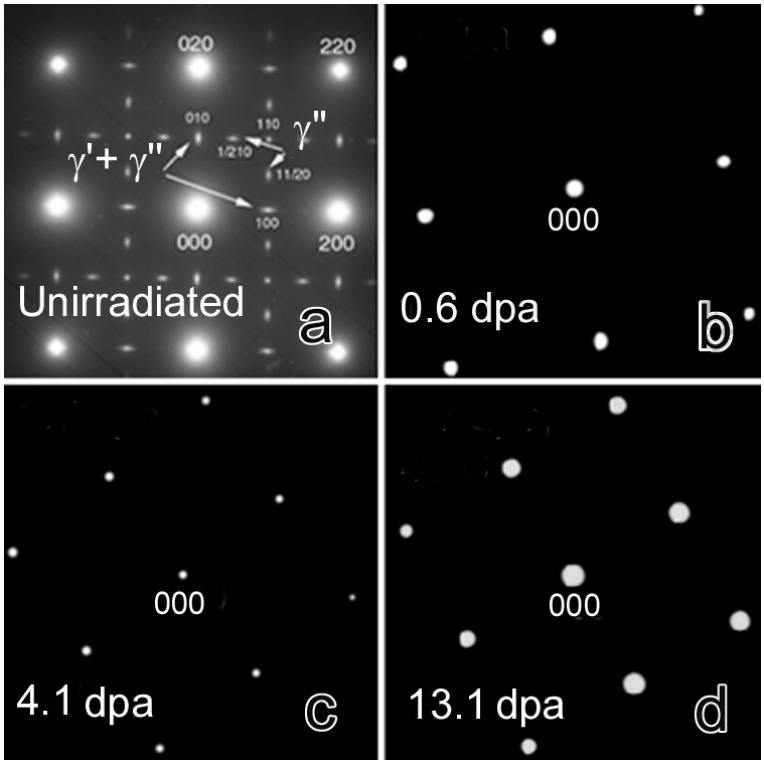

Fig. 7. [0 0 1] selected-area electron diffraction patterns from Alloy 718: (a) showing γ' and γ'' reflections; (b), (c), (d) showing disappearance of γ' and γ'' reflections after irradiation.

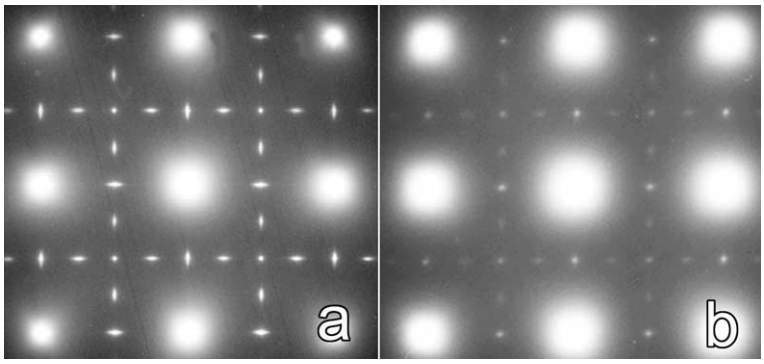

Fig. 8. [1 0 0] electron diffraction patterns of Alloy 718: (a) unirradiated; (b) ~0.1 dpa, 72°C.

black spots were visible in addition to the precipitates (Fig. 10). The loops produced distinctive satellite spots around the fundamental matrix spots on diffraction patterns. The satellite spots arise from extended diffraction streaks (relrods) perpendicular to the four sets of {1 1 1} planes. Similar intensities of satellite diffraction spots from the four ⟨1 1 1⟩ relrods indicated essentially equal Frank-loop populations on all four {1 1 1} planes. DF images of the loops taken with such satellite spots revealed faulted Frank loops, as shown in Fig. 11. 100 loops from each DF TEM micrograph were measured to obtain an average loop diameter. The average loop diameter was ~10.6 nm at 3.8 dpa and ~23.7 nm at 13.4 dpa. Fig. 12 shows the [0 1 1] lattice image of an edge-on faulted Frank loop at 1.5 dpa.

The possibility of cavity formation was investigated in near-kinematic conditions (Fresnel contrast). Several

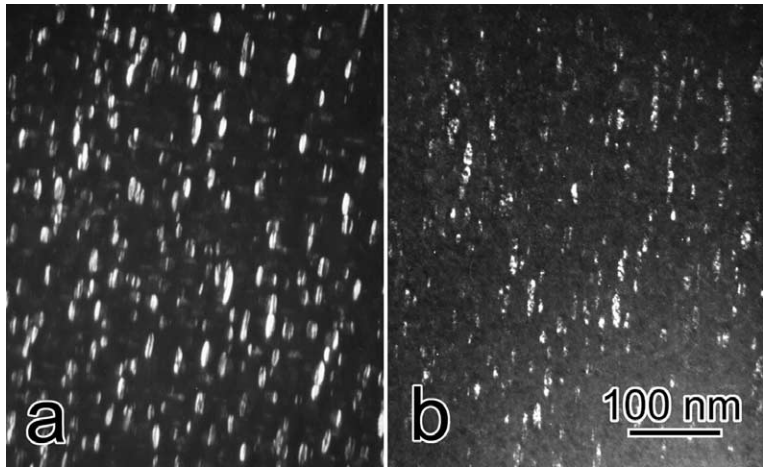

Fig. 9. DF images from close to [1 0 0] zone axis in Alloy 718, $g = (0\,1\,0)$ $(\gamma' + \gamma'')$ precipitate DF images: (a) unirradiated; (b) ~0.1 dpa, 72°C.

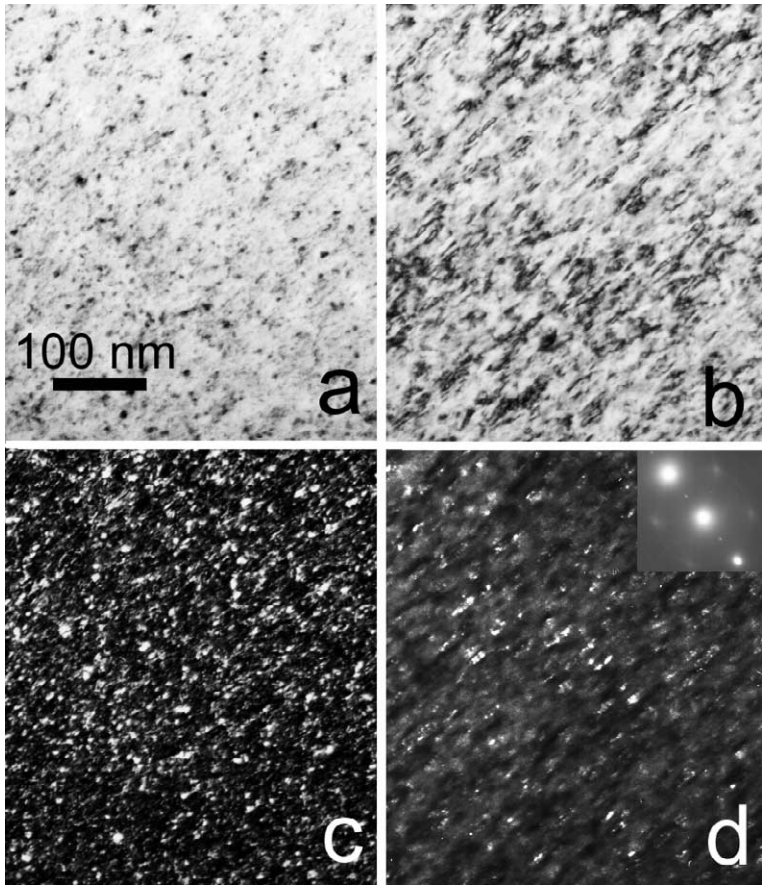

Fig. 10. Black-spot damage in Alloy 718 (~0.1 dpa): (a) $g = 200$ $s \gg 0$ BF contrast; (b) $g = 200$ $s > 0$ BF contrast; (c) $g = 200$ $g/4g$ weak-beam image; (d) precipitate DF contrast. All images are from the same area of the grain.

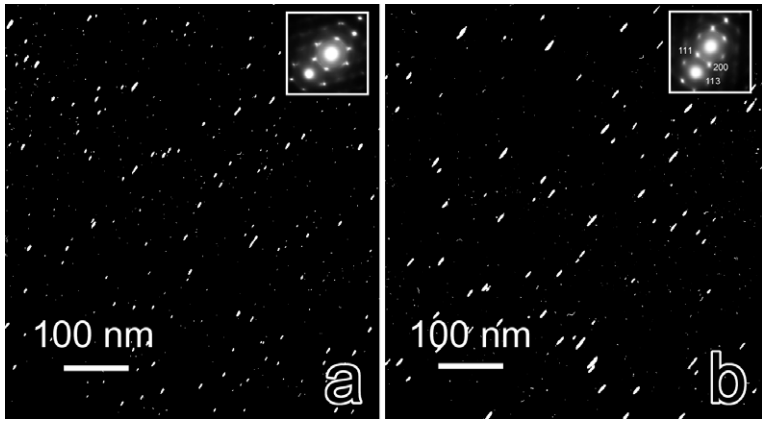

Fig. 11. Faulted Frank loops in Alloy 718, imaged with one of the ⟨1 1 1⟩ relrods in: (a) 3.8; (b) 13.4 dpa samples. Corresponding diffraction patterns are shown as insets.

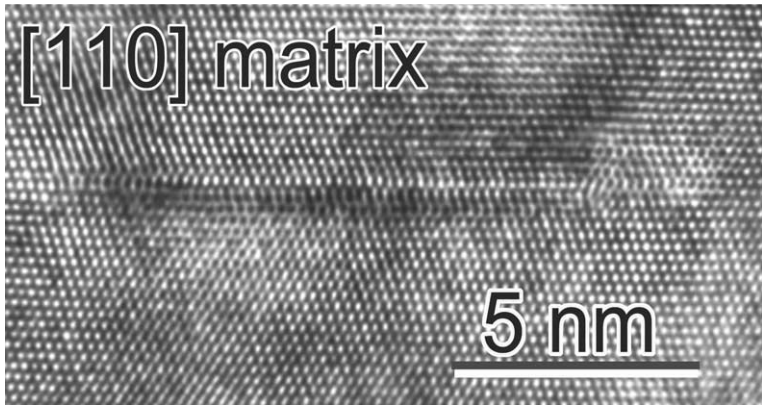

Fig. 12. High-resolution electron micrograph of radiation-induced Frank loop in irradiated Alloy 718, 1.5 dpa [0 1 1] lattice image.

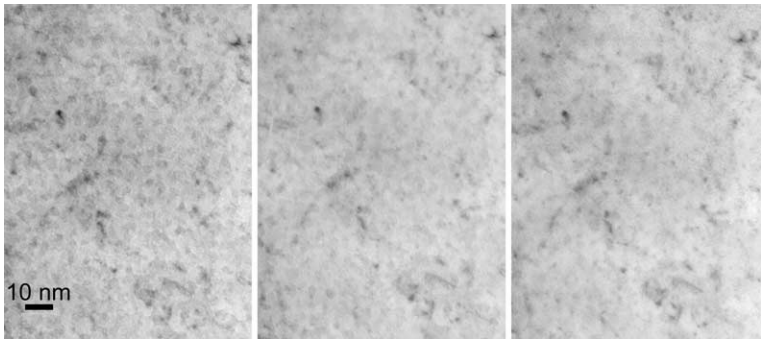

Fig. 13. Kinematic through-focal image series from 13.4 dpa Alloy 718. From left to right: under-focus, focus and over-focus, showing that no cavities are observed in the matrix.

through-focal images were taken, as shown in Fig. 13. Examination of the samples irradiated to the higher dose (13.4 dpa) showed that no cavity formation had occurred, down to a resolution of ~1 nm [10].

4. Discussion

A most interesting and complex evolution of both microstructure and mechanical properties occurred in

Alloy 718. The stability of γ' and γ'' phases in Alloy 718 is affected by irradiation with mixed spectra of protons and spallation neutrons at low temperatures (32–55°C), even at doses as low as 0.6 dpa. All evidence for these phases had disappeared from the electron diffraction patterns after proton-induced doses ranging from 0.6 through 13.4 dpa. The microstructure of irradiated Alloy 718 was dominated instead by black-spot damage and larger faulted loops at all dose levels, the average loop size increasing with increasing dose. These microstructural trends might, at first thought, suggest a very different evolution of mechanical behavior from what is actually observed in tensile tests [2] and microhardness measurements [11]. If all the age-hardening precipitates were completely lost by 0.6 dpa, one would expect an initial softening of the material. This would then be followed by hardening, as the loop density and sizes increased. In practice, however, the opposite trend was seen in the evolution of mechanical behavior [2]. After an initial hardening, the yield stress decreases with increasing dose; in other words, the material softens for all doses $\geqslant 0.6$ dpa.

Carsughi et al. [11] have investigated a similar softening behavior (based on microhardness data) in Inconel 718 after irradiation with 800 MeV protons to $\sim$10 dpa at temperatures that were somewhat variable and higher, but below 250°C. The disappearance of γ' and γ'', and the presence of η-phase (which can form as a product of overaging in irradiated or unirradiated 718) were reported. The presence of η-phase was suggested by Carsughi to be a possible cause of softening of the material. In the present study at lower temperatures, however, no evidence of η-phase was found, although faulted Frank loops were imaged with the $\langle 1\,1\,1\rangle$ relrods (see Fig. 10). Identification of η-phase in the work of Carsughi et al. [11] is thought to be questionable, possibly resulting from misidentification of faulted loops as η-phase.

Between $\sim$0.6 and $\sim$13.4 dpa, in the present study, lack of γ' and γ'' precipitate reflections in diffraction patterns gave the initial impression that the precipitates disappeared at very low ($\leqslant$0.6 dpa) doses. To investigate further the behavior of these precipitates, Alloy 718 samples irradiated to $\sim$0.1 dpa with only spallation neutrons were examined. In these samples, γ' and γ'' precipitates were found to be losing their superlattice intensity, becoming only faintly visible in electron diffraction patterns, and difficult to image with precipitate reflections. The next available dose for examination was $\sim$0.6 dpa (protons and spallation neutrons). The precipitate reflections were totally absent from diffraction patterns by 0.6 dpa, and no additional spots from new phases were observed. This finding strongly suggests that γ' and γ'' disappeared well before 0.6 dpa. The question then becomes how to interpret this disappearance.

One interpretation would be that the γ' and γ'' have dissolved, but this is inconsistent with the changes in mechanical behavior, as explained above. It is also difficult to envisage complete dissolution occurring at such a low dose, in the absence of significant thermal diffusion. Another interpretation, however, would be that the precipitates have only lost much of their ordered structure, with the local solute concentrations remaining.

The loss of order may result from the displacement cascades that occur during radiation damage [12]. At low irradiation temperatures, thermal diffusion is very limited, and cascade-induced mixing may become the most important short-range transport mechanism. Under 800 MeV proton irradiation, very large cascades are thought to be produced. As a result of cascade formation, atomic mixing occurs, along with interstitial and vacancy production [13]. Such processes might not be detrimental to solution-hardened material, but, in the case of ordered intermetallic phases, extensive mixing and defect formation will lead to extensive disordering. Complete dissolution by 0.6 dpa would lead to a softening that is inconsistent with the initial increase in hardening observed [2]. It is therefore proposed that the precipitates become disordered, but are retained in the range of 0.0 and $\sim$0.6 dpa as regions of locally high solute concentration that can still harden the material similar to GP (Guinier–Preston) zones. Thus, for low doses there is no significant softening associated with the disorder, and the concurrent development of black-spot damage leads to an overall increase in hardness.

Alloy 718 exhibited a partial softening between $\sim$0.6 and $\sim$13.4 dpa. This is attributed to gradual redistribution of the solutes as the dose increases over this range. The observed mechanical behavior might be explained as follows. The early study of Silcock et al. [14] on GP zones in binary aluminum–copper alloys showed that the main contribution to hardness comes not from the ordering of GP zones, but from segregation of solute atoms to the GP zones. Therefore, by analogy, the disordering of γ' and γ'' alone should not remove all of the hardening associated with the precipitates. Subsequent dissolution of the solute concentrations could, however, produce substantial softening that might be sufficient to outweigh hardening due to further formation of Frank loops, and hence results in a net softening effect at doses $>$0.6 dpa.

A drastic loss of ductility was observed in Alloy 718 at all dose levels examined. The early loss of ductility may be attributed to radiation-induced hardening, as loops are formed. What is perhaps more surprising, however, is that there is no recovery of ductility as softening of the material occurs at higher doses. Some increase in ductility might be expected to accompany the decreases in yield stress that are seen as dose increases beyond 0.6 dpa, but this is not the case. A possible explanation for this is as follows. In the unirradiated condition the γ' and γ'' precipitates are hard particles

that induce Orowan hardening. At low dose, they become disordered, and start to become shearable by dislocations. This allows strain localization (dislocation channeling), which gives total loss in uniform elongation and less hardening [15]. Increasing dose reinforces strain localization and the loss in elongation does not recover. It must also be remembered, however, that substantial amounts of helium and hydrogen accumulated in the samples during the LANSCE irradiations [4,5]. TEM examination revealed a complete absence of cavity formation in Alloy 718, even though levels of ~1830 appm helium and ~5000 appm hydrogen were reached at 13.4 dpa. It appears that there is insufficient mobility of helium atoms in the temperature range 32–72°C to allow nucleation and growth of bubbles or voids. Thus, the helium and hydrogen must be dispersed on a very fine scale within the material. It is thought that these high gas levels within the lattice also contribute to the continued brittleness of the material, even as the yield strength and hardness decrease. Indeed, the hydrogen in solution may also contribute to the rapidity with which ductility is lost.

5. Conclusions

Based on the combined results of mechanical testing, gas retention, and microstructural evolution, the following conclusions can be drawn.

By ~0.1 dpa, images of γ' and γ'' precipitates lose some of their intensity, and show discontinuous contrast, indicating disordering, while γ' and γ'' superlattice reflections are still faintly visible in the electron diffraction patterns. No new phases are precipitated from γ' and γ''. A dose of ~0.1 dpa is thought to be sufficient to induce partial disordering of the precipitates at ~72°C.

All evidence of the γ' and γ'' precipitates disappears from the diffraction patterns by 0.6 dpa. If complete dissolution of the precipitates were to occur, the material should soften, but, on the contrary, Alloy 718 hardens up to ~0.6 dpa. It is proposed here that the precipitates are essentially disordered by 0.6 dpa, but that the solutes they contained are not yet fully redistributed into the matrix. Thus, the precipitates retain the majority of their original hardening contribution.

At low doses, the dominant microstructural features are black-spot damage and remnants of the γ' and γ'' phases. Together, the black-spot damage and remains of the precipitates result in a net hardening up to 0.6 dpa, since both are obstacles to dislocation movement.

At doses between ~0.6 and ~13 dpa, the observable microstructure of Alloy 718 is dominated by only black-spot damage and larger faulted Frank loops. No evidence of any new phase was found in the diffraction patterns.

At doses between 0.6 and ~13 dpa, Alloy 718 softens somewhat. The gradual softening is attributed to mixing-induced redistribution of the solutes from the former γ' and γ'' precipitates as the dose increases.

In spite of the large levels of retained helium and hydrogen, no cavities are produced at doses as high as ~13 dpa. The gas atoms must be dispersed in the matrix as single atoms or very small complexes.

Acknowledgements

This work was supported by the US Department of Energy under the Accelerator Production of Tritium Program at Los Alamos National Laboratory. Pacific Northwest National Laboratory is operated for USDOE by Battelle Memorial Institute.

References

[1] S.A. Maloy, W.F. Sommer, R.D. Brown, J.E. Roberts, J. Eddleman, E. Zimmerman, G.J. Willcutt, in: M.S. Wechler, L.K. Mansur, C.L. Snead, W.F. Sommer (Eds.), in: Proceedings of the Symposium on Materials for Spallation Neutron Sources, TMS, Warrendale, PA, 1998, p. 35.

[2] M.L. Hamilton, F.A. Garner, M.B. Toloczko, S.A. Maloy, W.F. Sommer, M.R. James, M.R. Louthan Jr., J. Nucl. Mater. 283–287 (2000) 418.

[3] S.A. Maloy, M.R. James, G.J. Willcutt, W.F. Sommer, W.R. Johnson, M.R. Louthan Jr., M.L. Hamilton, F.A. Garner, in: S.T. Rosinski, M.L. Grossbeck, T.R. Allen, A.S. Kumar (Eds.), Effects of Radiation on Materials, 20th International Symposium, ASTM STP 1405, American Society for Testing and Materials, West Conshohocken, PA, 2002, in press.

[4] B.M. Oliver, F.A. Garner, S.A. Maloy, W.F. Sommer, P.D. Ferguson, M.R. James, in: S.T. Rosinski, M.L. Grossbeck, T.R. Allen, A.S. Kumar (Eds.), Effects of Radiation on Materials, 20th International Symposium, ASTM STP 1405, American Society for Testing and Materials, West Conshohocken, PA, 2002, in press.

[5] F.A. Garner, B.M. Oliver, L.R. Greenwood, M.R. James, P.D. Ferguson, S.A. Maloy, W.F. Sommer, these Proceedings, p. 66.

[6] M.R. James, S.A. Maloy, W.F. Sommer, P.D. Ferguson, M.M. Fowler, K. Corzine, in: Second International Topical Meeting on Nuclear Applications of Accelerator Technology, Gatlinburg, TN, 20–23 September, 1998, p. 605.

[7] G.J. Willcutt, S.A. Maloy, M.R. James, J. Teague, D.A. Siebe, W.F. Sommer, P.D. Ferguson, in: Second International Topical Meeting on Nuclear Applications of Accelerator Technology, Gatlinburg, TN, 20–23 September, 1998, p. 254.

[8] D.F. Paulonis, J.M. Oblak, D.S. Duvall, Trans. ASM 62 (1969) 611.

[9] J.M. Oblak, D.F. Paulonis, D.S. Duvall, Metall. Trans. 5 (1974) 143.
[10] B.H. Sencer, G.M. Bond, F.A. Garner, M.L. Hamilton, B.M. Oliver, L.E. Thomas, S.A. Maloy, W.F. Sommer, M.R. James, P.D. Ferguson, J. Nucl. Mater. 283–287 (2000) 324.
[11] F. Carsughi, H. Derz, P. Ferguson, G. Pott, W. Sommer, H. Ullmaier, J. Nucl. Mater. 264 (1999) 78.
[12] R.E. Stoller, G.R. Odette, B.D. Wirth, J. Nucl. Mater. 251 (1997) 49.
[13] D.J. Bacon, A.F. Calder, F. Gao, J. Nucl. Mater. 251 (1997) 1.
[14] J.M. Silcock, T.J. Heal, H.K. Hardy, J. Inst. Met. 82 (1953–1954) 239.
[15] K. Farrell, private communication.